Accessing the Chain Length Dependence of the Termination Rate Coefficient for Disparate Length Radicals via Reversible Addition Fragmentation Chain Transfer Chemistry: A Theoretical Study

Tara M. Lovestead, Alexander Theis, Thomas P. Davis, Martina H. Stenzel, and Christopher Barner-Kowollik*

Centre for Advanced Macromolecular Design, School of Chemical Sciences and Engineering, The University of New South Wales, Sydney, New South Wales 2052, Australia

Received March 23, 2006; Revised Manuscript Received May 12, 2006

ABSTRACT: On the basis of the recently introduced reversible addition fragmentation chain transfer chain length dependent termination (RAFT−CLD−T) method, a novel approach is presented to access the termination rate coefficient for disparate length radicals, $k_t^{s,l}$. In-depth simulation is employed to validate this approach, which utilizes reversible addition fragmentation chain transfer (RAFT) chemistry to generate two nearly monodisperse chain length distributions with disparate average lengths, *s* and *l*. These disparate length radicals are generated by prepolymerizing a polyRAFT species to a chain length significantly greater than unity and subsequently progressing the polymerization of the polyRAFT species in the presence of a suitable RAFT agent of initial chain length 1. The present study demonstrates that the chain length dependence of the termination rate coefficient for disparate length radicals can be obtained accurately regardless of the extent of the prepolymerization period of the polyRAFT species, the input kinetic parameters, and whether the geometric or the harmonic mean approximation is assumed for the relationship between k_t and the individual radical chain lengths *s* and *l*. Thus, for the first time a facile and accurate method for quantification of $k_t^{s,l}$ is validated theoretically allowing for a complete characterization of free radical termination processes for disparate length radicals.

Introduction

Improving the understanding of the termination processes during free radical polymerizations (FRP) has been an ongoing objective over the past few decades.[1−18] While, at first, the termination reaction may appear to be a relatively simple process, the attainment of accurate and reliable rate coefficients has proved to be anything but straightforward and the scientific community has produced many reviews that focus solely on FRP termination processes and the variety of methods that allow for its quantification.[9,14−18] The termination process is inherently complex to characterize because it is a bimolecular reaction that requires translational diffusion of the center-of-masses of large macroradicals and subsequent segmental rearrangement of their chain ends before chemical reaction can occur. Thus, the termination rate depends on all factors that influence the mobility of the radical chain, e.g., viscosity, monomer to polymer conversion, and degree of polymerization. Most importantly, the diffusion-controlled nature of the termination reaction implies that the termination rate coefficient, k_t, is a function of the chain length of the terminating radicals.

Recently, the difficulties and complexities associated with the accurate and reliable determination of k_t have been reviewed thoroughly.[17] Characterization of the termination reaction is complicated further by the fact that there are almost as many techniques to measure the conversion and chain length dependence of k_t as there are research groups working in the field. Of the seventeen experimental techniques reviewed,[17] living free radical polymerization (LFRP) techniques such as nitroxide-mediated FRP, atom-transfer FRP, and reversible addition fragmentation chain transfer (RAFT) FRP are helping to improve the more conventional techniques in addition to spawning new techniques for facile and reliable quantification of the conversion and chain length dependence of k_t in both stationary and nonstationary experiments.

LFRP is characterized by a nearly monodisperse chain length distribution that grows uniformly with reaction time, i.e., monomer consumption (eq 1).[17,19]

$$i(t) = \frac{\int_0^t R_p(t)\,dt}{[\mathrm{LFRP}]_0} + 1 \qquad (1)$$

Ideally, the chain length, *i*, depends solely on the amount of monomer consumed, $\int_0^t R_p(t)\,dt$, where $R_p(t)$ is the polymerization rate as a function of time, and $[\mathrm{LFRP}]_0$ is the LFRP-mediating agent concentration at $t = 0$.

All of the established LFRP techniques are capable of controlling the chain length distribution throughout the polymerization and have been utilized extensively both in academia and in industry as tools for generating complex macromolecular structures, see for example refs 20−28. However, RAFT polymerization offers the advantage (provided that the initial RAFT agent is chosen judiciously) of nominal impact on the radical concentration and, concomitantly, the propagation and termination rates.[29] This unique attribute of RAFT FRP renders it ideal for aiding current and novel experimental techniques aimed at obtaining a better understanding of chain length dependent termination during FRP.

While many readers are already intimately familiar with the reactions, for clarity of discussion, Scheme 1 presents a typical RAFT-mediated FRP mechanism. Reaction I entails a two-step initiation mechanism, where the generation of initiating radicals, $I^\bullet$, (Ia) depends on the rate coefficient, k_d, and on the initiator efficiency, *f*. Additionally, the formation of primary radicals, $P_1^\bullet$, (Ib) depends on the initiation rate coefficient, k_i. Reactions II and IV are unique to RAFT polymerizations and represent the preequilibrium where the initial RAFT agent is transformed

* Corresponding author. E-mail: camd@unsw.edu.au. Fax: 61.2.9385.6250. Telephone: 61.2.9385.4331.

10.1021/ma060646x CCC: $33.50
Published on Web 06/27/2006

Scheme 1. Basic Reactions Describing the Reversible Addition Fragmentation Chain Transfer (RAFT) Process[a]

I. INITIATION

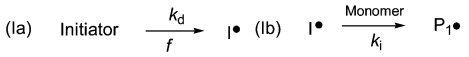

II. PRE-EQUILIBRIUM

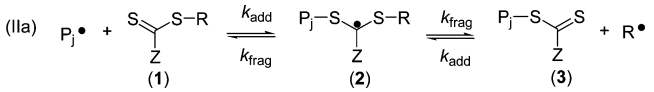

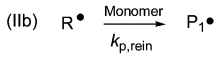

III. PROPAGATION

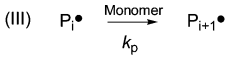

IV. CORE EQUILIBRIUM

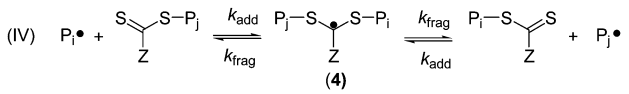

V. TERMINATION

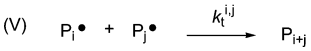

[a] Note that in an effectively working RAFT process, $i \approx j$.

into macroRAFT agent and the core equilibrium where the polyRAFT species grows uniformly with monomer to polymer conversion. The pre-equilibrium also entails monomer addition to the RAFT agent-derived radicals, R•, which proceeds with a rate coefficient, $k_{p,rein}$. The pre-equilibrium and the core equilibrium are governed by the magnitude of the addition and fragmentation rate coefficients (k_{add} and k_{frag}). Reactions III and V represent the conventional FRP propagation and termination reactions, respectively; however, only termination by combination is taken into account (i.e., the termination rate coefficient for disproportionation is equal to 0). In addition, the depicted RAFT mechanism accounts for the chain length dependence of the termination rate coefficient, $k_t^{i,j}$ (reaction V). Note that in an effectively functioning RAFT process $i \approx j$ and that under certain circumstances, and when employing very stabilized RAFT agents, additional side reactions as well as a persistent radical effect can be present in the RAFT process. These complexities of the RAFT mechanism will not be reiterated in the present study as an ideal RAFT process involving fast fragmentation of the intermediate radical species is assumed.[29,30]

Two promising methods have been developed that exploit RAFT FRP as a tool for determining k_t as a function of polymerization time (i.e., as a function of radical chain length, $k_t^{i,i}$, where i is the radical chain length, eq 1); the (stationary) CAMD-invented RAFT chain length dependent termination (RAFT−CLD−T) technique[31−36] and the (nonstationary) single pulse−pulsed laser polymerization−RAFT (SP−PLP−RAFT) procedure.[37] The SP−PLP−RAFT technique is based on the classical single pulse−pulsed laser polymerization (SP−PLP) technique, which uses on-line near-infrared spectroscopy to monitor monomer conversion in the dark after an initiating laser pulse to obtain the ratio of the rate coefficients, k_t/k_p, (eq 2).[38,39]

$$\frac{[M](t)}{[M]_0} = (2k_t[P^\bullet]_0 t + 1)^{-k_p/2k_t} \tag{2}$$

Here, [M] is the monomer concentration, $[M]_0$ is the initial monomer concentration prior to applying the laser pulse, $[P^\bullet]_0$ is the radical concentration of radicals generated by the laser pulse, t is the time, and k_p is the chain length-independent propagation rate coefficient, which may be determined independently via pulsed laser polymerization combined with size-exclusion chromatography (PLP−SEC).[9] In the absence of chain transfer, the classical SP−PLP technique uses a single laser pulse to generate a nearly monodisperse radical population with an average chain length that grows linearly with time according to $i \approx k_p[M]t$, and thus, the conversion dependence of k_t is possible to assess.[12,38] More complex and model-based analyses of an SP−PLP trace can yield the potential chain length dependence of k_t (see for example refs 12 and 39) Further, electron spin resonance (ESR) spectroscopy has also been combined with SP−PLP into ESR−SP−PLP to ascertain the chain length dependence of k_t.[40,41]

The recent combination of conventional SP−PLP and the RAFT−CLD−T method (i.e., the SP−PLP−RAFT technique),[37,42] which utilizes a RAFT agent to minimize the change in the radical population's average chain length following the laser pulse, allows the classical, chain length-independent, form of the monomer consumption eq 2 to be utilized. This technique has been realized experimentally and has been validated via modeling on the RAFT-mediated butyl acrylate polymerization in a recent collaborative effort.[42]

The RAFT−CLD−T technique affords the advantage over SP−PLP−RAFT in that it is based on the direct and experimentally nondemanding measurement of the polymerization rate as a function of time, $R_p(t)$ (eq 3). Thus, RAFT−CLD−T characterizes the chain length dependence of k_t via a stationary technique that is experimentally very simple. Recently, both RAFT−CLD−T and SP−PLP−RAFT have been demonstrated to give consistent results.[42]

$$R_p(t) = -\frac{d[M]}{dt} = k_p[M][P^\bullet] \tag{3}$$

The polymerization rate is related to the termination rate coefficient via eq 4, which indicates that the radical concentration at any point in time depends on the initiation rate, R_i, minus the termination rate, R_t.[1,43,44]

$$\frac{d[P^\bullet]}{dt} = 2f k_d[I] - 2k_t[P^\bullet]^2 \tag{4}$$

The factor of 2 is necessary because initiator decomposition results in 2 initiating fragments. Solving eq 4 for k_t provides the termination rate coefficient averaged as a function of time (eq 5), when the initiator decomposition rate coefficient (eq 6), the propagation rate coefficient, as well as the initiator efficiency are available.[34] For a detailed analysis of the prerequisite parameters needed to employ eq 5 the reader is referred to ref 36.

$$\langle k_t \rangle(t) = \frac{2fk_d[I]_0 e^{-k_d t} - \dfrac{d\left(\dfrac{R_p(t)}{k_p([M]_0 - \int_0^t R_p(t)\,dt)}\right)}{dt}}{2\left(\dfrac{R_p(t)}{k_p([M]_0 - \int_0^t R_p(t)\,dt)}\right)^2} \tag{5}$$

$$R_i(t) = -\frac{d[I]}{dt} = k_d[I] \tag{6}$$

Note that eq 5 makes no assumption of a steady state radical concentration and in its given form is only valid for monomers forming insignificant quantities of less reactive midchain radicals.[36] The strength of the RAFT−CLD−T method lies in not only the facile experimental access to the polymerization rate (for example via calorimetric rate measurements) but also the ability to control the chain length distribution as a function of time and monomer conversion.

At any point in time, the average termination rate coefficient (eq 5) correlates with the microscopic chain length dependent termination kinetic coefficient, $k_t^{i,j}$, via eq 7.[10,45]

$$\langle k_t \rangle = \frac{\sum_{i=1}^{n}\sum_{j=1}^{n} k_t^{i,j}[P_i^\bullet][P_j^\bullet]}{\left(\sum_{i=1}^{n}[P_i^\bullet]\right)^2} \quad (7)$$

Here, the numerator is the total termination rate that takes into account a different k_t possible for each combination of radical chains; n is the longest radical chain length that undergoes termination; and $\Sigma_{i=1}^{n}$ $[P_i^\bullet]$ is the total radical concentration. Even though a truly monodisperse chain length distribution is never achieved, RAFT chemistry allows for a nearly monodisperse chain length distribution (i.e., $i \approx j$) and eq 7 simplifies to show that the average termination kinetic coefficient at each time point is equal to $k_t^{i,i}$. As mentioned above, RAFT chemistry is used to assess the termination rate coefficient for *disparate* length radicals. In this manuscript, i and j refer to the nearly equivalent length chains within a distribution and s and l refer to the "short" and "long" average chain length distributions, respectively. As has been performed in many studies, a simple power-law equation may be used to determine the extent that k_t depends on the radical chain length, where the exponent α is an indicator for the magnitude of the chain length dependence (eq 8).

$$k_t^{s,s} = k_{t0}(s \cdot s)^{-\alpha/2} \quad (8)$$

In principle, eq 1 provides the kinetic chain length for a RAFT-mediated FRP where $[LFRP]_0$ is equal to the RAFT agent concentration at $t = 0$, $[RAFT]_0$. However, the kinetic chain length depends on the RAFT agent's kinetic parameters (i.e., the magnitude of the addition and fragmentation rate coefficients in the pre- and core equilibrium), and thus, eq 9 more accurately describes the chain length as a function of time

$$s(t) = \frac{M_n^{ex}}{MW_{RU}} \quad (9)$$

where, M_n^{ex} is the experimentally determined number-average molecular weight and MW_{RU} is the molecular weight of the monomer repeat unit. Originally, the RAFT−CLD−T technique was exemplified on styrene[29,31] and was later applied successfully to map the chain length dependence of k_t for methyl acrylate,[32] butyl acrylate,[42] dodecyl acrylate,[34] and methyl methacrylate.[46] Additionally, the RAFT−CLD−T methodology has been used to map simultaneously the dependence of k_t on both chain length and monomer conversion for methyl acrylate[33] and vinyl acetate[35] polymerizations. In the present study, the versatility of RAFT-mediated FRP as a tool for obtaining a better understanding of termination processes during FRP is revealed.

This method is based on the original RAFT−CLD−T method, which is modified for the parallel polymerization of two RAFT species of disparate average chain length, s and l. Modeling is a useful tool for developing a method and is used here to demonstrate that reliable information about $k_t^{s,l}$ can be obtained directly from measurement of the polymerization rate. This novel procedure and analytical approach are examined in detail theoretically with the goal of aiding future experimental efforts to elucidate $k_t^{s,l}$.

Results and Discussion

Model Development. RAFT chemistry affords the advantage of controlling the chain length distribution without affecting the reaction kinetics (i.e., in theory—chain length dependent termination itself aside—displaying the same radical concentration as observed in corresponding conventional free radical systems). The feasibility and challenges of using RAFT chemistry to develop an expanded RAFT−CLD−T method to characterize the termination rate coefficient for disparate length radicals (denoted s and l in the following), $k_t^{s,l}$, is explored via simulation. To the best of our knowledge, this novel method and analytical approach is the first reported and studied theoretically that quantifies $k_t^{s,l}$. De Kock and co-workers proposed another method that uses PLP, the "TR-echo-PLP" method; however, they offered neither theoretical nor experimental justification.[2]

To quantify $k_t^{s,l}$, two distributions of radical chains with disparate average chain lengths are generated by accounting for two complete sets of the reactions presented in Scheme 1. Chains from different distributions are denoted using the superscript s or l, respectively, for the shorter or longer chain species, for example, $[P_i^{s\bullet}]$ represents a radical of arbitrary chain length i from the distribution of shorter length radical chains, s. Thus, initiation, propagation, macroRAFT agent and polyRAFT species generation, as well as termination, occurs for each distribution according to the above kinetic equations and reaction Scheme 1. In addition, core equilibrium and termination occurs between either the "long" (l) or "short" (s) chain polyRAFT species and reactive radical, respectively (see Scheme 2). To reiterate the nomenclature employed throughout this study, within a given RAFT distribution the individual chain lengths are denoted i and j and are assumed to be approximately equivalent; chains belonging to different distributions are denoted s and l.

Figure 1 illustrates the desired simultaneous growth of two polyRAFT species of disparate average chain lengths. Initially, at $t = 0$, only the "long" polyRAFT species is present, e.g., a distribution with an initial average chain length, l, equal to 43 is present. At $t = 0$ a second RAFT agent is administered and two distributions of polyRAFT species are evident at 1880 s. Both the "long" and "short" chain length distributions shift toward higher degrees of polymerization with increasing polymerization time.

To provide insight into termination kinetics between disparate length radical chains, the program package PREDICI, version 6.36.1, on an Athlon 64 × 2 Dual Core Processor 3800+ IBM-compatible computer, was utilized. A RAFT-mediated FRP is simulated until its polyRAFT species has achieved a certain pre-set chain length. Subsequently, a function that is inherent in the PREDICI package that allows the user to change the concentration of a low molecular weight reactant mid-simulation is employed to add initiator and RAFT agent to start the generation of the second, "short", polyRAFT species. Thus,

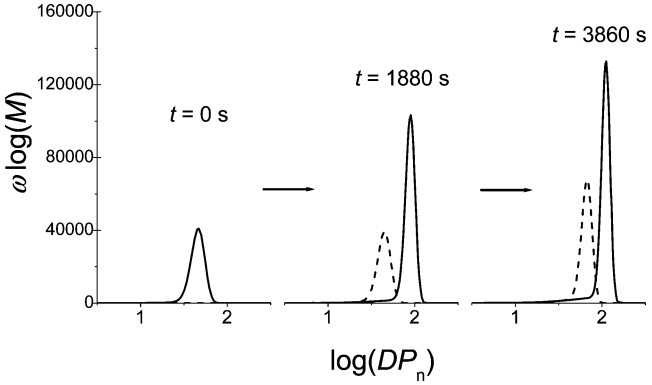

Figure 1. Simulated (radical) MWD evolution of the two RAFT species having an initial average chain length, *l*, equal to 43 (—) and 0 (···) is presented at $t = 0$, 1880, and 3860 s. The rate coefficients and other parameters relevant for the simulation are collated in Table 1. The simulation has been parametrized on the example of a styrene bulk polymerization at 80 °C. All φ input values, $\varphi^{s,s}$, (and $\varphi^{l,l}$) or $\varphi^{s,l}$, are set to 0.16 and the geometric mean is used (see analytical procedures section for a definition of φ and the geometric mean). Note that the concentrations of the individual radical distributions associated with each polyRAFT distribution are identical.

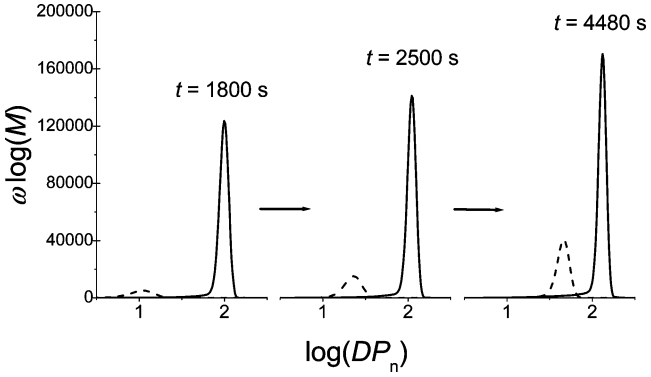

Figure 2. The simulated (radical) MWD evolution of the two RAFT species having an initial average chain length, *l*, equal to 83 (—) and 0 (···) is depicted at $t = 1800$, 2500, and 4480 s, where time here includes the prepolymerization time to achieve an initial polyRAFT species ($l = 83$). The rate coefficients and other parameters relevant for the simulation are collated in Table 1. The simulation has been parametrized on the example of a styrene bulk polymerization at 80 °C. All φ input values, $\varphi^{s,s}$, (and $\varphi^{l,l}$) or $\varphi^{s,l}$, are set to 0.16 and the geometric mean is used (see analytical procedures section for a definition of φ and the geometric mean).

Scheme 2. Core Equilibrium and Termination Reactions for Two Disparate Distributions of Radical Chains Generated via RAFT-Mediated FRP

I. CORE EQUILIBRIUM

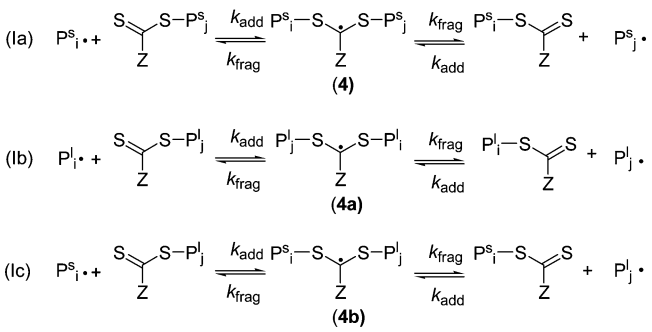

II. TERMINATION

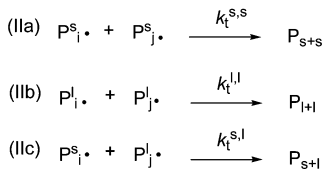

$t = 0$ in Figure 1 effectively corresponds to $t = 620$ s simulation time, i.e., the time necessary to generate a polyRAFT species having an average length, *l*, equal to 43. The latter times presented in Figure 1 are 620 s less than the total simulation time.

RAFT agents are administered at preselected time points solely to generate disparate average length polyRAFT distributions. Then the two distributions are monitored by PREDICI, which differentiated them based on whether they were generated from RAFT agent administered at time zero or at a time greater than zero. Interestingly, since the core equilibrium reaction Ic mixes the chains generated at early time points with the shorter (younger) chains, short and long chains exist in each distribution independent of when the RAFT agent is administered. This mixing of the chains is not a problem experimentally as SEC differentiates chains based only on their size and not on the time point that the RAFT agent is introduced into the reaction. However, this mixing of the chains via the core equilibrium reaction results in the model predicting identical bimodal distribution for both polyRAFT species. This situation poses no problem unless the "short" and "long" chain distributions overlap because one would have to develop a criterion for how to separate the distributions (in order to obtain their individual degree of polymerization). However, we chose not to subjectively manipulate the model output and instead conducted all simulations without accounting for the cross exchange equilibrium reaction Ic in Scheme 2. This simplification does *not* impact the predicted reaction kinetics and/or kinetic chain lengths as has been verified extensively and allows for MWD predictions analogous to that which a SEC experiment would provide.

To probe further the model's ability to simulate the MWD evolution of the polyRAFT species, Figure 2 presents the case when the "long" polyRAFT species is allowed to grow for 1400 s, i.e., to an initial average chain length, *l*, equal to 83. Figure 2 indicates that increasing the chain length of the first polyRAFT distribution (i.e., increasing the simulation time prior to administering the second RAFT agent) increases the difference in the average chain length of each distribution, and thus, significantly decreases the overlap between the "short" and "long" chain length distributions.

As is evident from Figures 1 and 2, a monodisperse chain length distribution is not achieved. However, once the initial RAFT agent is consumed (after approximately 3% conversion), the polydispersity of polyRAFT species remains below 1.4. Thus, the average chain length of the polyRAFT species, and concomitantly, the average chain length of the propagating radical distribution, *s* or *l*, is assumed to be equal to the ratio of the first moment to the zeroth moment of the MWD of the polyRAFT species (Figure 3). The simulation conditions presented here are identical to those employed in Figure 1.

Figure 3 indicates that at 20% of the monomer conversion the average chain length of the initial polyRAFT distribution is approximately 43. The addition of a second RAFT agent, which, in this case, occurs at 20% monomer conversion, causes a second shorter average chain length polyRAFT distribution to grow and decreases the rate at which the longer average chain length polyRAFT distribution grows (as is denoted in Figure 3 by a change in the slope for the long polyRAFT species).

CDV

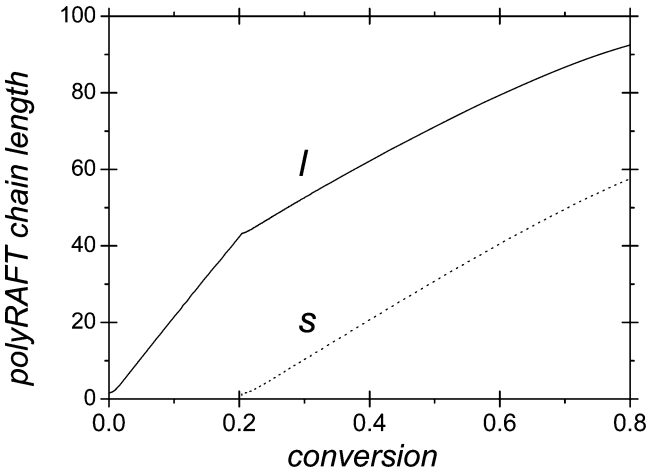

Figure 3. Average chain length of the prepolymerized polyRAFT species (*l*, —) and of the polyRAFT species that is initiated at $t = 620$ s (*s*, ···) as a function of conversion is presented as predicted via simulation at 80 °C. All φ input values, $\varphi^{s,s}$, (and $\varphi^{l,l}$) or $\varphi^{s,l}$, are set to 0.16 and the geometric mean is used (see analytical procedures section for a definition of φ and the geometric mean). The rate coefficients and other parameters relevant for the simulation are collated in Table 1.

Table 1. Input Parameters Used for the Kinetic Modeling of the RAFT-Mediated Free Radical Bulk Polymerization of Styrene at 80 °C[a]

k_d/s^{-1}	k_p	f	k_{add} [29]	k_{frag}/s^{-1} [29]	k_{t0}
1.36×10^{-4} [47]	663 [48]	0.713 [49]	5.0×10^5	1.0×10^5	1.0×10^7

k_i	$k_{p,rein}$	$[I]_0$	$[RAFT]_0$	$[Sty]_0$[29]	T/°C
$k_i \geq k_p$	$k_{p,rein} \geq k_p$	2.0×10^{-2}	4.0×10^{-2}	8.73	80

[a] All rate coefficients are given in L mol^{-1} s^{-1} and all concentrations are given in mol L^{-1} unless otherwise indicated.

Model Parameters. Knowledge of the average length of each polyRAFT distribution and the polymerization rate as a function of time provides all of the necessary information to directly determine the termination rate coefficient for disparate length radicals, $k_t^{s,l}$. The material properties, kinetic parameters, and rate coefficients for the RAFT-mediated FRP of styrene using 2,2′-azobisbutyronitrile (AIBN) as the initiator at 80 °C are utilized. To exemplify this method, styrene (Sty) was selected because it has been modeled extensively and its rate coefficients and material properties are readily available in the literature. The rate coefficients for initiator decompositions, k_d,[47] and propagation, k_p,[48] are available from the literature. The rate coefficient for termination at time equal to zero, k_{t0}, is not styrene specific and the procedure works for various k_{t0} values. An estimation of the initiator efficiency, f,[49] for AIBN has also been detailed. Values for the addition and fragmentation rate coefficients, k_{add} and k_{frag},[29] are more difficult to assess; however, when the RAFT agent does not induce significant rate retardation and inhibition phenomena it can be assumed safely that fragmentation is a fast processes. In here, a fragmentation rate coefficient of 10^5 s^{-1} [29] has been employed as done before in the context of the RAFT−CLD−T method. Additionally, the rate coefficients for initiation and for monomer addition to the RAFT agent derived radical, R•, $k_{p,rein}$, do not impact the model output as long as they are selected to be greater than k_p. All parameters used in the kinetic model are listed in Table 1.

Analytical Procedure. Accounting for the termination events between propagating radicals from distributions of disparate average chain length requires that the relationship between the macroscopic average k_t and microscopic chain length dependent k_t (eq 7) be examined carefully. Assuming that the two distributions are represented adequately by their respective average chain length, eq 10 provides the relationship for the average termination rate coefficient and the termination rate coefficients for two "short" chains, $k_t^{s,s}$, two "long" chains, $k_t^{l,l}$, and one "short" and one "long" chain, $k_t^{s,l}$.

$$\langle k_t \rangle = \frac{k_t^{s,s}[P_s^\bullet]^2 + 2k_t^{s,l}[P_s^\bullet][P_l^\bullet] + k_t^{l,l}[P_l^\bullet]^2}{([P_l^\bullet] + [P_l^\bullet])^2} \tag{10}$$

Here, $[P_s^\bullet]$ and $[P_l^\bullet]$ are the concentration of "short" and "long" radical chains, respectively. When equal concentrations of reacting species exist (i.e., $[P_s^\bullet] = [P_l^\bullet]$) eq 10 simplifies to eq 11.

$$\langle k_t \rangle = \frac{1}{4}k_t^{s,s} + \frac{1}{2}k_t^{s,l} + \frac{1}{4}k_t^{l,l} \tag{11}$$

Equal concentrations of reacting species are achieved by employing equal concentrations of RAFT agent (for the polyRAFT and initial RAFT species) resulting in a simple relationship for the dependence of $k_t^{s,l}$ on the average termination rate coefficient, and the termination kinetic coefficients for equal length radical chains (eq 12). While this assumption may seem counterintuitive due to the fact that CLD−T involves small radicals terminating faster than long radicals, which should lead to concentration differences between polyRAFT species with disparate average chain lengths, the RAFT-mediated polymerization process is a steady state process which means that terminating radicals are replaced by newly generated radicals. Thus, as long as there is initiator present in the reacting system, each population of polyRAFT species remains constant. In addition, in order to obtain equal concentrations of propagating "short" and "long" radicals, the addition and fragmentation reactions in the RAFT process are assumed to be chain length independent.

$$k_t^{s,l} = 2\langle k_t \rangle - \frac{1}{2}k_t^{s,s} - \frac{1}{2}k_t^{l,l} \tag{12}$$

Accounting for the termination of disparate radical chain lengths requires modification of the power-law relationship given by eq 8 to yield eq 13. To test the robustness of this method, a further function to determine the dependence of the termination rate coefficient on disparate chain lengths is utilized (eq 14). In eqs 13 and 14, the extent or magnitude of the chain length dependence of the short−long termination is expressed via the exponent φ (identical to the role that α has in eq 8). Analogous equations for short−short and long−long termination are employed also.

$$k_t^{s,l} = k_{t0}(s \cdot l)^{-\varphi/2} \tag{13}$$

$$k_t^{s,l} = k_{t0}\left(\frac{2s \cdot l}{s + l}\right)^{-\varphi} \tag{14}$$

These equations are known as the geometric (eq 13) and harmonic (eq 14) mean approximation and have been used extensively in the past to model the chain length dependence of the termination rate coefficient.[16,45,50,51] These equations are advantageous because they are easy to rearrange, providing an analytical solution for the extent that the termination rate coefficient depends on chain lengths, φ.

To distinguish between termination events taking place between chains of approximately identical size (*ss* or *ll*) and

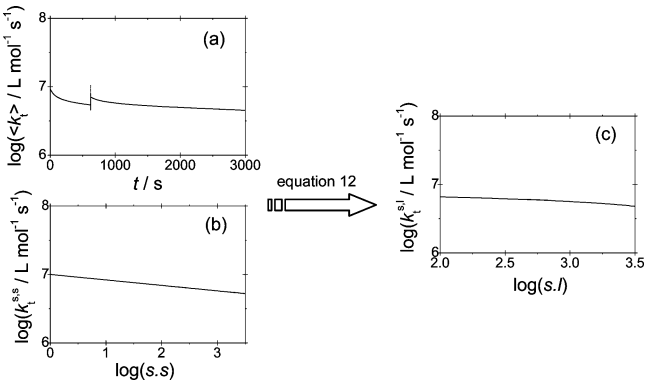

Figure 4. Log plot of the average termination kinetic coefficient, $\langle k_t \rangle$, vs polymerization time (a), along with double−log plots of the short−short, $k_t^{s,s}$, and short−long, $k_t^{s,l}$, termination rate coefficients vs the products of the radical chain lengths terminating (b and c, respectively) are presented for the simulated RAFT-mediated styrene polymerization at 80 °C with a polyRAFT species that has been prepolymerized to an average chain length, l, equal to 43. All φ input values, $\varphi^{s,s}$, (and $\varphi^{l,l}$) or $\varphi^{s,l}$, are set to 0.16, the geometric mean is used, and data up to 65% conversion is presented. Note that when $\varphi^{s,s}$ and $\varphi^{l,l}$ are equal that the model predicts the same $k_t^{s,s}$ and $k_t^{l,l}$ for equivalent chain lengths. The rate coefficients and other parameters relevant for the simulation are collated in Table 1.

those of disparate size (*sl* and *ls*), we denote the extent of similar size termination (within macroradicals associated with the same polyRAFT distribution) $\varphi^{s,s}$ (or $\varphi^{l,l}$) and the extent of disparate size termination (within macroradicals associated with different polyRAFT distributions) $\varphi^{s,l}$ (or $\varphi^{l,s}$). The extent that the termination rate coefficient depends on disparate length radicals, $\varphi^{s,l}$, is obtained via construction of a double−log plot of either eq 13 or eq 14, where the $k_t^{s,l}$ values are obtained from eq 12. Figure 4 illustrates eq 12, that is, how the average termination rate coefficient ($\langle k_t \rangle$, deduced from eq 5 from the rate of polymerization data, Figure 4a) and the $k_t^{s,s}$ (deduced from prior knowledge of the extent to which similar size radical chains terminate, $\varphi^{s,s}$, and thus, $\varphi^{l,l}$, Figure 4b) combine to provide the termination rate coefficient for disparate length radicals, $k_t^{s,l}$, (Figure 4c). The simulation conditions presented here are identical to those employed in Figure 1.

Figure 4a also reveals that the average termination rate coefficient increases when the second RAFT agent and initiator are added, which generates a younger (shorter) chain polyRAFT species that terminates more readily than the older (longer) chain length polyRAFT species (born at $t = 0$). The addition of the second RAFT agent and initiator is instantaneous and the termination rate, and concomitantly the initiation and polymerization rates (see Figures 6 and 7), achieve steady state in one second of simulated polymerization time, after which k_t is predicted to decrease with increasing polymerization time, i.e., increasing chain length (Figure 4).

The extent that the termination rate coefficient depends on disparate length radicals, $\varphi^{s,l}$, is determined via fitting the slope of the double−log plot of $k_t^{s,l}$ vs the product of the chain lengths when employing eq 13. Note that when eq 14 is employed that the double−log plot will present $k_t^{s,l}$ vs $2sl/(s + l)$. The data are fit from approximately 3% conversion after the second RAFT agent is administered to approximately 85% monomer conversion or until the data no longer exhibits a linear relationship for the combination of the "short" and "long" chain lengths relevant to either eq 13 or eq 14 vs polymerization time.

To illustrate the analytical approach for characterizing $\varphi^{s,l}$, Figure 5 presents an example of a double-log plot of eq 13. Both the model predictions and the slope of the best linear fit

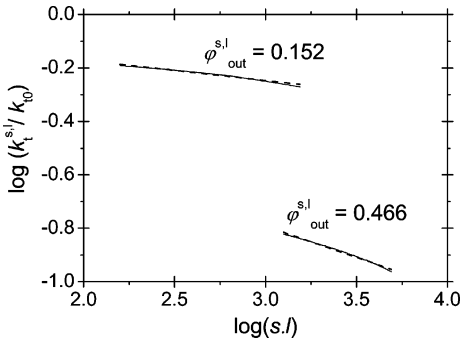

Figure 5. Double−log plot of $k_t^{s,l}$ normalized by k_{t0} vs the product of the average chain length of the two polyRAFT species (of disparate chain length s and l) is presented as predicted by the simulated polymerization of styrene, RAFT agent, and an average polyRAFT species of initial average chain length equal to 43. Two cases are presented: one simulation where $\varphi^{s,l} = 0.16$, and one where $\varphi^{s,l} = 0.50$. The dashed line is the best linear fit to the data (continuous line). The slope of the linear fit is equal to $-\frac{1}{2}\varphi^{s,l}_{out}$ (see eq 13) and gives the extent of $k_t^{s,l}$'s chain length dependence. In both cases all parameters except $\varphi^{s,l}$ are equal and $\varphi^{s,s}$ (and $\varphi^{l,l}$) is 0.16.

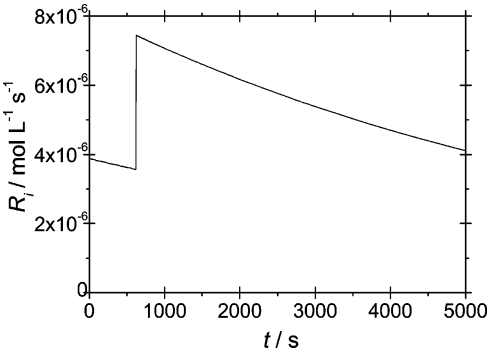

Figure 6. Initiation rate vs polymerization time presented as predicted via simulation of a RAFT-mediated styrene polymerization at 80 °C with a polyRAFT species that has been prepolymerized to an initial average chain length, l, equal to 43. All φ input values, $\varphi^{s,s}$, $\varphi^{l,l}$, and $\varphi^{s,l}$, are set to 0.16 and the geometric mean is used. The rate coefficients and other parameters relevant for the simulation are collated in Table 1.

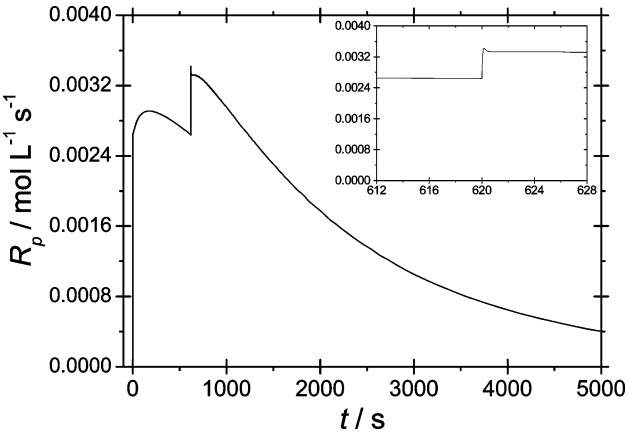

Figure 7. Polymerization rate vs time presented as predicted via simulation of a RAFT-mediated styrene polymerization at 80 °C with a polyRAFT species that has been prepolymerized to an initial average chain length, l, equal to 43. All φ input values, $\varphi^{s,s}$, (and $\varphi^{l,l}$) or $\varphi^{s,l}$, are set to 0.16 and the geometric mean is used. The rate coefficients and other parameters relevant for the simulation are collated in Table 1.

are presented, indicating that the method returns $\varphi^{s,l}_{out}$ (i.e., the method deduced input parameter for the extent of the chain length dependence) equal to 0.152 and 0.466. These values agree

Table 2. $\varphi^{s,l}{}_{out}$ Presented As Determined from the Slope of the Best Linear Fit Using the Geometric Mean (Eq 13) to the Simulated Data for the RAFT-Mediated Styrene Polymerization at 80 °C[a]

$\varphi^{s,s},\varphi^{l,l}$	$\varphi^{s,l}$	$i^{prepolymer}$	slope of best linear fit	$\varphi^{s,l}{}_{out}$
0.16	0.16	43	−0.076	0.152
0.16	0.16	63	−0.076	0.152
0.16	0.16	83	−0.078	0.155
0.16	0.16	99	−0.076	0.152
0.16	0.16	118	−0.081	0.162
0.16	0.16	133	−0.080	0.160
0.16	0.16	144	−0.082	0.164
0.5	0.5	43	−0.233	0.466
0.5	0.5	64	−0.198	0.395
0.5	0.5	85	−0.229	0.458
0.5	0.5	105	−0.232	0.464
0.16	0.5	84	−0.220	0.440
0.5	0.16	85	−0.073	0.146

[a] Various chain lengths for the polyRAFT species, $i^{prepolymer}$, and input values for the scaling exponent for short−short, $\varphi^{s,s}$ (and long−long, $\varphi^{l,l}$), and short−long, $\varphi^{s,l}$, termination are presented.

Table 3. $\varphi^{s,l}{}_{out}$ Presented As Determined from the Slope of the Best Linear Fit Using the Harmonic Mean (Eq 14) to the Simulated Data for the RAFT-Mediated Styrene Polymerization at 80 °C

$\varphi^{s,s},\varphi^{l,l}$	$\varphi^{s,l}$	$i^{prepolymer}$	slope of best linear fit	$\varphi^{s,l}{}_{out}$
0.16	0.16	43	−0.146	0.146
0.16	0.16	63	−0.145	0.145
0.16	0.16	84	−0.154	0.154
0.16	0.16	99	−0.145	0.145
0.16	0.16	118	−0.153	0.153
0.16	0.16	133	−0.167	0.167
0.16	0.16	144	−0.172	0.172
0.5	0.5	43	−0.474	0.474
0.5	0.5	64	−0.425	0.425
0.5	0.5	85	−0.430	0.430
0.5	0.5	105	−0.358	0.358
0.16	0.5	83	−0.467	0.467
0.5	0.16	85	−0.140	0.140

[a] Various chain lengths for the polyRAFT species and input values for the scaling exponent for short−short, $\varphi^{s,s}$ (and long−long, $\varphi^{l,l}$), and short−long, $\varphi^{s,l}$, termination are collated.

well with the model input values of $\varphi^{s,l}$ 0.16, and 0.5, respectively. Interestingly, when $\varphi^{s,l}$ is 0.5, the plot exhibits nonlinear behavior. This nonlinearity is due to the high initiation and concomitant termination rate, which results in more polydisperse populations. Reducing the initiation rate decreases the termination rate, generating more monodisperse populations that yield linear plots, i.e., improve the method's accuracy. However, the higher initiation condition is presented here because it represents more accurately the necessary condition for obtaining experimentally reliable rate information, e.g., when using differential scanning calorimetry (DSC). In both cases, all parameters except $\varphi^{s,l}$ are equal and $\varphi^{s,s}$ (and $\varphi^{l,l}$) is 0.16.

Model Validation. Tables 2 and 3 clearly demonstrate that the method's ability to predict $\varphi^{s,l}{}_{out}$ within reasonable accuracy does not depend on the extent of prepolymerization of the polyRAFT species, the $\varphi^{s,s}$, (and $\varphi^{l,l}$) or $\varphi^{s,l}$ input values, and/or whether the geometric or the harmonic mean is employed. Interestingly, when the harmonic mean is used (Table 3) and the termination rate coefficient has a strong chain length dependence (i.e., the scaling exponent φ is 0.5) the method's predictive capability decreases as is evident for a $\varphi^{s,l}{}_{out}$ value equal to 0.358. When chain length dependent termination is important one would expect that the concentration of the shorter length species will deplete more rapidly than the concentration of the longer length species. Additionally, k_t decreases less with increasing chain length (or combination of chain lengths) when the harmonic mean vs the geometric mean is used. Since the analytical technique is based on the assumption of equal concentration of reacting species (an assumption necessary for the simplification of eq 10), the model's predictive capability may weaken for very strong chain length dependence and/or increasing difference in each distribution's average chain length coupled with a very high termination rate coefficient. However, Table 2 reveals that when the difference in the reacting species chain length is increased the methods performance improves.

To illustrate the model further, Figures 6 and 7 present the polymerization and initiation rates as functions of time for an example case when a polyRAFT species has been prepolymerized to an average chain length, l, equal to 43, all φ input values, $\varphi^{s,s}$, (and $\varphi^{l,l}$) or $\varphi^{s,l}$, are set to 0.16, and the geometric mean is applied (see the first entry in Table 2). Adding initiator at 620 s increases the overall initiation rate (see Figure 6) from 3.6×10^{-6} to 7.4×10^{-6} mol L^{-1} s^{-1} and, concomitantly, the polymerization rate from 2.6×10^{-3} to 3.4×10^{-3} mol L^{-1} s^{-1} (see Figure 7). Note that the polymerization rate does not increase with the square root of the initiation rate and that classically the polymerization rate is expected to increase by $\sqrt{2}$ to 3.7×10^{-3} mol L^{-1} s^{-1}. This deviation from classical kinetics is due to the importance of chain length dependent termination. Thus, the newly initiated "short" chains terminate more readily than the older "long" chains, which results in an greater than expected increase in the termination rate (see Figure 4) and subsequent less than classically expected rise in the polymerization rate. The insert to Figure 7 reveals the initial increase in the polymerization rate in greater detail.

Figure 6 also presents the overall initiation rate, that is, the sum of the initiation rate for each of the two simultaneously occurring polymerizations. While equal initial initiator concentrations are always used the prepolymerization period necessary to generate the polyRAFT species with initial average chain length greater than one depletes some initiator. Thus, at $t =$ 620 s, R_i is less than $2R_{i0}$ (the value that is expected if no initiator is consumed during the prepolymerization process).

Potential Experimental Realization. We have demonstrated theoretically that the RAFT−CLD−T method has potential to assess the termination rate coefficient for radicals of disparate size. The next frontier is experimental quantification of $k_t^{s,l}$ for a variety of monomer systems. While the model implementation of the modified RAFT−CLD−T method is successful for establishing the robustness and feasibility of the novel procedure and analytical approach, some issues need to be addressed prior to implementation of this procedure into laboratory practice. To begin, adding RAFT agent and initiator at a well-defined point during a calorimetric rate experiment (carried out, e.g., in a differential scanning calorimeter) may not be feasible. Instead, we suggest carrying out this approach in two steps. First, the polyRAFT species is generated and its MWD characterized via SEC to ensure that an adequate chain length has been achieved. Second, the resulting polymerization rate of the reaction mixture containing monomer, initiator, new initial RAFT agent, as well as the prepolymerized polyRAFT species is monitored. Care should be taken with regard to the choice of the length of the prepolymerized RAFT species. Selecting an initial polyRAFT species that is too short will inevitably lead to an overlap with the short chain distribution and it will be highly difficult to assess individual M_n for each of the growing distributions as a function of reaction time. Additionally, selecting a polyRAFT species that is initially too long may result in more rapid depletion of the shorter species and invalidation

of the assumption of equal concentrations of reacting species at high monomer to polymer conversions. On the basis of the model projection of this study, it seems feasible to have an initial degree of polymerization of the prepolymer of greater than 80 (see Figure 2). Notwithstanding experimental measurement of the individual M_n of each distribution, it is still possible to assume an ideal average molecular weight evolution (as given by eq 1) for each polyRAFT (and thus, macroradical) distribution. Such an approach may indeed be feasible in cases where the RAFT agent/monomer system behaves ideally or close to ideally. Further, it remains to be established in an experimental context whether the signal-to-noise ratio in the polymerization rate measurements is sufficient to allow a treatment of the data as suggested in here. Provided that the signal-to-noise ratios are sufficient and on the basis of our experience in determining $k_t^{i,i}$ via the RAFT−CLD−T method, it seems likely that the data may be analyzed successfully via the modified RAFT−CLD−T method.

Conclusions

The application of RAFT-mediated FRP to control the chain length distribution throughout the polymerization with minimal impact on the kinetics has greatly advanced the quantification of chain length dependent termination rate coefficients. In the present theoretical study, a facile experiment for the determination of the chain length dependence of the termination rate coefficient for disparate length radicals is theoretically validated. A model that simulates the RAFT-mediated FRP of styrene at 80 °C was developed that demonstrates how RAFT chemistry can be used to generate disparate radical chain length distributions for quantification of $k_t^{s,l}$. Simulation reveals that the chain length dependence of the termination rate coefficient for disparate length radicals is obtained accurately for a range of different average "short" and "long" chain length polyRAFT distributions. Additionally, the method is accurate when either the geometric or the harmonic mean approximation is assumed for the relationship between k_t and the individual radical chain lengths s and l. In conclusion, a facile and novel method for quantification of $k_t^{s,l}$ is validated theoretically.

Acknowledgment. We are grateful for financial support from the Australian Research Council (ARC) in the form of a Discovery Grant (to C.B.-K. and M.H.S.). T.P.D. acknowledges a Federation Fellowship (ARC). We thank Dr. Leonie Barner and Mr. Istvan Jacenyik for their excellent management of CAMD.

References and Notes

(1) Allen, P. E. M.; Patrick, C. R. *Macromol. Chem.* **1961**, *47*, 154−167.
(2) de Kock, J. B. L.; Klumperman, B.; van Herk, A. M.; German, A. L. *Macromolecules* **1997**, *30*, 6743−6753.
(3) North, A. M.; Reed, G. A. *J. Am. Chem. Soc.* **1961**, *83*, 9−870.
(4) Benson, S. W.; North, A. M. *J. Am. Chem. Soc.* **1962**, *84*, 953−940.
(5) Mahabadi, H.; O'Driscoll, K. F. *Macromolecules* **1977**, *10*, 55−58.
(6) Soh, S. K.; Sundberg, D. C. *J. Polym. Sci., Polym. Chem. Ed.* **1982**, *20*, 1345−1371.
(7) Soh, S. K.; Sundberg, D. C. *J. Polym. Sci., Polym. Chem. Ed.* **1982**, *20*, 1299−1313.
(8) Mahabadi, H. *Macromolecules* **1991**, *24*, 606−609.
(9) Buback, M.; Gilbert, R. G.; Russell, G. T.; Hill, D. J. T.; Moad, G.; O'Driscoll, K. F.; Shen, J.; Winnik, M. A. *J. Polym. Sci., Part A: Polym. Chem.* **1992**, *30* (5), 851−863.
(10) Russell, G. T. *Macromol. Theory Simul.* **1995**, *4*, 497−517.
(11) Tobita, H. *Macromolecules* **1996**, *29*, 3073−3080.
(12) Buback, M.; Busch, M.; Kowollik, C. *Macromol. Theory Simul.* **2000**, *9*, 442−452.
(13) Olaj, O. F.; Kornherr, A.; Zifferer, G. *Macromol. Theory Simul.* **2001**, *10*, 881−890.
(14) Buback, M.; Egorov, M.; Gilbert, R. G.; Kaminsky, V. A.; Olaj, O. F.; Oskar, F.; Russell, G. T. *Macromol. Chem. Phys.* **2002**, *203*, 2570−2582.
(15) Olaj, O. F.; Kornherr, A.; Vana, P.; Zoder, M.; Zifferer, G. *Macromol. Symp.* **2002**, *182*, 15−30.
(16) Russell, G. T. *Austr. J. Chem.* **2002**, *55*, 399−414.
(17) Barner-Kowollik, C.; Buback, M.; Egorov, M.; Fukuda, T.; Goto, A.; Olaj, O. F.; Russell, G. T.; Vana, P.; Yamado, B.; Zetterlund, P. B. *Prog. Polym. Sci.* **2005**, *30*, 605−643.
(18) Smith, G. B.; Heuts, J.; Russell, G. T. *Macromol. Symp.* **2005**, *226*, 133−146.
(19) Fischer, H. *Chem. Rev.* **2001**, *101*, 3581−3610.
(20) Hawker, C. J.; Bosman, A. W.; Harth, E. *Chem. Rev.* **2001**, *101*, 3661−3688.
(21) Matyjaszewski, K.; Xia, J. *Chem. Rev.* **2001**, *101*, 2921−2990.
(22) Prescott, S. W.; Ballard, M. J.; Rizzardo, E.; Gilbert, R. G. *Austr. J. Chem.* **2002**, *55* (6&7), 415−424.
(23) Barner-Kowollik, C.; Davis, T. P.; Heuts, J. P. A.; Stenzel, M. H.; Vana, P.; Whittaker, M. *Polym. Sci., Part A: Polym. Chem.* **2003**, *41*, 365−375.
(24) Hao, X.; Heuts, J. P. A.; Barner-Kowollik, C.; Davis, T. P.; Evans, E. *J. Polym. Sci., Part A: Polym. Chem.* **2003**, *41*, 2949−2963.
(25) Mayadunne, R. T. A.; Jeffery, J.; Moad, G.; Ezio, R. *Macromolecules* **2003**, *36*, 1505−1513.
(26) Boyes, S. G.; Granville, A. M.; Baum, M.; Akgun, B.; Mirous, B. K.; Brittain, W. J. *Surf. Sci.* **2004**, *570* (1−2), 1−12.
(27) Hua, D.; Ge, X.; Bai, R.; Lu, W.; Pan, C. *Polymer* **2005**, *46*, 12696−12702.
(28) Perrier, S.; Takolpuckdee, P. *J. Polym. Sci., Part A: Polym. Chem.* **2005**, *43*, 5347−5393.
(29) Feldermann, A.; Stenzel, M. H.; Davis, T. P.; Vana, P.; Barner-Kowollik, C. *Macromolecules* **2004**, *37*, 2404−2410.
(30) Barner-Kowollik, C.; Buback, M.; Charleux, B.; Coote, M. L.; Drache, M.; Fukuda, T.; Goto, A.; Klumperman, B.; Lowe, A. B.; McLeary, J.; Moad, G.; Monteiro, M. J.; Sanderson, R. D.; Tonge, M. P.; Vana, P. *J. Polym. Sci., Part A: Polym. Chem.* **2006**, in press.
(31) Vana, P.; Davis, T. P.; Barner-Kowollik, C. *Macromol. Rapid Commun.* **2002**, *23*, 952−956 and references within.
(32) Theis, A.; Feldermann, A.; Charton, N.; Stenzel, M. H.; Davis, T. P.; Barner-Kowollik, C. *Macromolecules* **2005**, *38*, 2595−2605.
(33) Theis, A.; Davis, T. P.; Stenzel, M. H.; Barner-Kowollik, C. *Macromolecules* **2005**, *38*, 10323−10327.
(34) Theis, A.; Feldermann, A.; Charton, N.; Davis, T. P.; Stenzel, M. H.; Barner-Kowollik, C. *Polymer* **2005**, *46*, 6797−6809.
(35) Theis, A.; Davis, T. P.; Stenzel, M. H.; Barner-Kowollik, C. *Polymer* **2006**, *47*, 999−1010.
(36) Theis, A.; Stenzel, M. H.; Davis, T. P.; Barner-Kowollik, C. Obtaining Chain Length Dependent Termination Rate Coefficients via Thermally Initiated RAFT Experiments: Current Status and Future Challanges. In *ACS Symposium Series on Living/Controlled Free Radical Polymerization*; Matyjaszewski, K., Ed.; American Chemical Society: Washington, DC, 2006; Vol. 944, pp 486−500.
(37) Buback, M.; Junkers, T.; Vana, P. *Macromol. Rapid Commun.* **2005**, *26*, 796−802.
(38) Buback, M.; Kowollik, C. *Macromolecules* **1998**, *31*, 3211−3215.
(39) Buback, M.; Egorov, M.; Feldermann, A. *Macromolecules* **2004**, *37*, 1768−1776.
(40) Buback, M.; Egorov, M.; Junkers, T.; Panchenko, E. *Macromol. Rapid Commun.* **2004**, *25*, 1004−1009.
(41) Buback, M.; Müeller, E.; Russell, G. T. *J. Phys. Chem. A* **2006**, *110*, 3222−3230.
(42) Junkers, T.; Theis, A.; Buback, M.; Davis, T. P.; Stenzel, M. H.; Vana, P.; Barner-Kowollik, C. *Macromolecules* **2005**, *38*, 9497−9508.
(43) Russell, G. T.; Gilbert, R. G.; Napper, D. H. *Macromolecules* **1993**, *26*, 3538−3552.
(44) Mahabadi, H. *Macromolecules* **1985**, *18*, 1319−1324.
(45) Smith, G. B.; Russell, G. T. *Macromol. Theory Simul.* **2003**, *12*, 299−314.
(46) Johnston-Hall, G.; Theis, A.; Monteiro, M. J.; Davis, T. P.; Stenzel, M. H.; Barner-Kowollik, C. *Macromol. Chem. Phys.* **2005**, *206*, 2047−2053.
(47) Van Hook, J. P.; Tobolsky, A. V. *J. Am. Chem. Soc.* **1958**, *80*, 779.
(48) Buback, M.; Gilbert, R. G.; Hutchinson, R. A.; Klumperman, B.; Kuchta, F.-D.; Manders, B. G.; O'Driscoll, K. F.; Russell, G. T.; Schweer, J. *Macromol. Chem. Phys.* **1995**, *196*, 3267−3280.
(49) Buback, M.; Huckestein, B.; Kuchta, F.-D.; Russell, G. T.; Schmid, E. *Macromol. Chem. Phys.* **1994**, *195*, 2117−2140.
(50) Olaj, O. F.; Kornherr, A.; Zifferer, G. *Macromol. Theory Simul.* **1998**, *7*, 501.
(51) Olaj, O. F.; Zifferer, G. *Macromolecules* **1987**, *20*, 850.

MA060646X